



Inspired and Stabilized by Nature: Ribosomal Synthesis of the Human Voltage Gated Ion Channel (VDAC) into 2D-Protein-Tethered Lipid Interfaces

Journal:	<i>Biomaterials Science</i>
Manuscript ID:	BM-ART-03-2015-000097.R1
Article Type:	Paper
Date Submitted by the Author:	06-Jun-2015
Complete List of Authors:	<p>Damiati, Samar; King Abdulaziz University, Department of Biochemistry Zayni, Sonja; University of Natural Resources and Life Sciences, Vienna, Department of NanoBiotechnology Schrems, Angelika; University of Natural Resources and Life Sciences, Department of Nanobiotechnology Kiene, Elisabeth; AGES, Chopineau, Joel Sleytr, Uwe; University of Natural Resources and Life Sciences, Vienna, Department of NanoBiotechnology; University of Natural Resources and Applied Life Sciences, Universität für Bodenkultur Wien Schuster, Bernhard; University of Natural Resources and Life Sciences, Vienna, Department of NanoBiotechnology Sinner, Eva-Kathrin; Universität für Bodenkultur Wien, Institute for Nanobiotechnology</p>



Journal Name

ARTICLE

Inspired and Stabilized by Nature: Ribosomal Synthesis of the Human Voltage Gated Ion Channel (VDAC) into 2D-Protein-Tethered Lipid Interfaces

Received 00th January 20xx,
Accepted 00th January 20xx

DOI: 10.1039/x0xx00000x

www.rsc.org/

Samar Damiaty^{a,b}, Sonja Zayni^a, Angelika Schrems^{a†}, Elisabeth Kiene^{a††}, Uwe B. Sleytr^c; Joël Chopineau^d, Bernhard Schuster^a and Eva-Kathrin Sinner^{a*}

We present an elegant synthesis and reconstitution approach for functional studies of voltage responsive membrane proteins. For such studies, we propose a planar architecture of an S-layer-supported lipid membrane as a suitable matrix for presenting unmodified membrane protein species, here we focus on the voltage-dependent anion channel (VDAC) from human mitochondria. The presented cell-free strategy, in which VDAC proteins are synthesized *via* the ribosomal context of a cell lysate, into a membrane structure, offers a great advantage in the study of such subtle membrane proteins over the conventional, cell-based synthesis approach in terms of reproducibility. The material – assay combination is superior over cell – culture related synthesis and purification approaches as here, we bypass by a one-step synthesis procedure the complex cell culture, expression and purification endeavours and, moreover, the protein of interest never has to be detergent solubilized and had been synthesized *de novo*. We provide here a detailed description from the allover procedure and our first results, describing in detail the cell – free synthesis and robustness of such material – assay combination: functional VDAC protein species embedded in a planar membrane architecture and ready for electrochemical characterization.

Introduction

Integral membrane proteins are amphiphilic macromolecules that play vital roles in cells. The structure, function, and properties of membrane proteins have been the subject of extensive research. Biomimetic model lipid membranes have long been used to reconstitute membrane proteins for structural-functional analysis.

In addition to their use in fundamental studies regarding self-assembly (1,2), synthetic lipid membrane architectures are highly attractive for several industrial applications as synthetic membranes pose the potential to translate fragile amphiphilic

molecules such as membrane proteins, into devices. For example, drug–membrane interactions are an important consideration in the pharmaceutical industry because these interactions affect the efficacy and safety of new products (3,4). Moreover, studying membrane proteins in an environment that mimics *in vivo* conditions will facilitate drug design and development (3,5).

Such research and application endeavour would be enabled if the target molecules – namely the membrane proteins – would be translated from the complexity of a cell into a planar membrane context. Solid-supported lipid membranes are one of the most successful synthetic, planar membrane architectures described in literature over the past decades. Supported membranes, which comprise a bilayer assembly of phospholipids on a solid substrate, enable the investigation of protein and membrane using a wide range of surface-sensitive analytical techniques (5,6). Based on their electrochemical properties, reproducibility, and robustness, we present quasi-crystalline bacterial cell surface-layer (S-layer) proteins as a suitable material of a highly organized protein layer that effectively organizes the lipid-protein membrane on a solid inorganic support material (7–9). S-layer proteins do recrystallize as a crystalline monomolecular layer on a broad spectrum of solid substrates, including gold- and silicon dioxide-coated surfaces, in order to form a 5–10-nm-thick

^a Institute for Synthetic Bioarchitectures, Department of NanoBiotechnology, University of Natural Resources and Life Sciences, Muthgasse 11, Vienna 1190, Austria.

^b Department of Biochemistry, King Abdulaziz University, Jeddah 21465, Saudi Arabia.

^c Institute for Biophysics, Department of NanoBiotechnology, University of Natural Resources and Life Sciences, Muthgasse 11, Vienna 1190, Austria.

^d Institute Charles Gerhardt, UMR 5253 CNRS/ENSCM/UM2/UM1, Montpellier – France.

† Present address: Sysmex Austria GmbH, Odoakergasse 34–36, Vienna 1160, Austria.

†† Present address: Austrian Agency for Health and Food Safety (AGES), Vienna, Austria.

* Author to whom correspondence should be addressed; E-Mail: eva.sinner@boku.ac.at

highly porous lattice (8,10-13). Numerous studies have demonstrated that S-layer recrystallization induces nanopatterned membrane fluidity and extended longevity on adjacent membrane layers (14-16). In general, the self-assembly properties S-layer structures permit their easy preparation on solid supports to form a tether for lipid bilayer structure *via* vesicle fusion (14,15) which we call S-layer supported Lipid membrane (SsLM).

In this study, we developed a strategy for membrane protein insertion into such synthetic membrane system SsLM using the cell-free (*ex vivo*) protein expression system (16,17), eliminating the need for time- and effort-intensive cell culture-based protein expression and purification protocols. Cell-free systems offer a powerful tool for small-scale protein synthesis and are a promising alternative that overcomes the limitations of cell-based (*in vivo*) systems. Furthermore, cell-free systems are “open” and are therefore accessible, facilitating adjustments in reaction conditions and the introduction and control of labels and modifications. The additional advantages of cell-free systems include the elimination of the toxic or inhibitory effects of the proteins to the host cells and the generation of soluble, folded and functional proteins in sufficient amounts, enabling the incorporation of non-natural or chemically modified amino acids into the expressed protein at desired positions and the expression of both single genes and DNA libraries (18,19).

The human voltage-dependent anion channel (VDAC) represents a relevant membrane protein species. VDAC is comprised of 283 amino acids with an apparent molecular weight of 30 to 35 kDa. VDAC is predominantly found in the outer mitochondrial membrane system, where it is responsible for the permeability of the membrane to ions and small hydrophilic molecules and also plays a central role in the mitochondrial apoptotic pathways (20-22). Based on functional expression studies performed in conventional bacterial expression systems, VDAC has been described to form a cylindrical channel with a diameter of 20 to 30 Å and a 19-stranded β -barrel in which the first and last strands are parallel and enclose an N-terminal α -helix (23,24). However, the presence of the small ligand nicotinamide adenine dinucleotide (NADH) regulates the gating function for metabolites in the mitochondrial outer membrane by binding to VDAC (25). The NADH-binding site for human VDAC is located at strands 17 and 18, comprising residues 235 to 245 (24). When reconstituted in artificial membranes, the VDAC protein forms a voltage-gated channel. The VDAC protein is in the open state at low membrane potentials (<10 mV) and switches to the closed state at high membrane potentials (20). The present study reports on the interaction of *in vitro* (cell-free) synthesized human VDAC protein with SsLM.

We demonstrate synthesis in a bacterial cell lysate, purification and subsequent fusion of the VDAC protein onto a readily prepared SsLM architecture, see Figure 1. Functionality of the *in vitro* generated VDAC was characterized in real time

via the method of quartz crystal microbalance with dissipation monitoring (QCM-D) in combination with electrochemical impedance spectroscopy (EIS). This method combination enables the measurement of the planar membrane architecture formation, the resulting membrane resistance and further on the impact of VDAC protein reconstitution and ligand response.

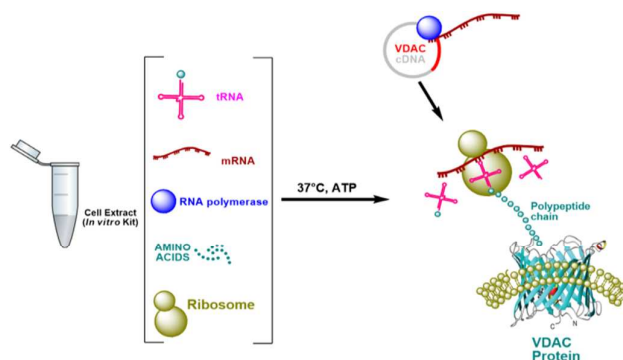


Figure 1: schematic image of cell free VDAC synthesis.

Results

Formation of the S-layer supported lipid membrane (SsLM)

The recrystallization of the S-layer protein and the formation of a lipid bilayer (schematically depicted in Fig. 2) was monitored by QCM-D by measuring changes in frequency and dissipation as a function of time (Fig. 3). The reassembly of S-layer protein from solution onto a gold-coated sensor (Fig. 2, step 1) resulted in a decrease in the frequency of $\Delta F \approx -100$ Hz and an increase in the dissipation of $\Delta D < 1 \times 10^{-6}$ (Fig. 3). These data are in good accordance with previously published studies (14,15). After the recrystallization of S-layer protein, the surface was rinsed with water to remove excess protein materials. S-layer protein was then activated with EDC, which reacted with the carboxyl groups on the S-layer proteins to form highly reactive O-acylisourea intermediates (Fig. 2 and 3, step 2).

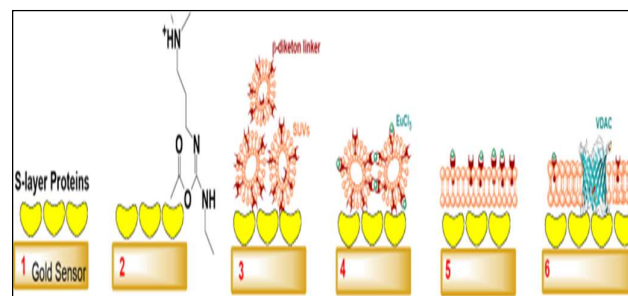


Figure 2: Schematic, step-by-step representation of the formation of the SsLM followed by incorporation of the VDAC protein. The VDAC NMR solution structure is adapted from Ref. 23.

Subsequently a solution of small unilamellar vesicles (SUVs) including Egg PC, DMPE, cholesterol, and a β -diketone linker

was injected. The SUVs bound via the amino groups of DMPE on the activated proteinaceous surface (Fig. 2, step 3) to form stable amide bonds (14,27). The addition of liposomes resulted in fusion – as we interpreted the significant decrease in the ΔF values (increasing mass load) and an increase in the ΔD values (increasing dissipative losses; Fig. 3).

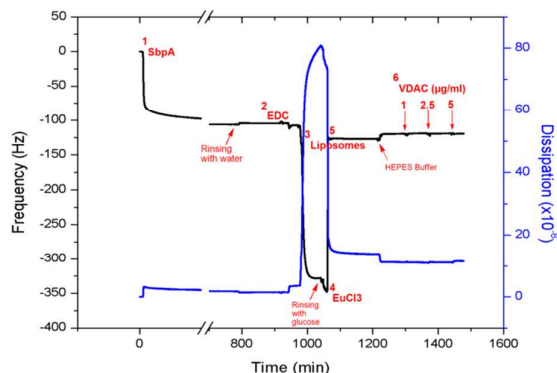


Figure 3: Changes in frequency and dissipation versus time during the formation of the SsLM and the reconstitution of VDAC proteoliposomes at various concentrations at 25°C. QCM-D data were recorded at the 7th overtone.

In the next step, europium ions (Eu^{3+}) were added to the bound SUVs to induce cross-linking of the SUVs (Fig. 2 and 3, step 4). The bilayer structure formed immediately after the addition of Eu^{3+} (Fig. 2 and 3, step 5) due to the formation of a coordinate complex between Eu^{3+} and β -diketone in a 1:2 ion-to-ligand ratio (14). Fusion is triggered when a complex of one Eu^{3+} and two or more ligands is formed between two adjacent vesicles (28,29). The rupture of liposomes results in the release of trapped water, thus altering the values of ΔF and ΔD . Water trapped inside and coupled to SUVs was detected as a mass gain during the adsorption of intact vesicles, whereas a mass loss due to water release was attributed to vesicle rupture and SsLM formation (Fig. 3). The obtained shift in frequency for the final lipid bilayer membrane was approximately 25 Hz, which is in good agreement with the reported QCM-D response for bilayer formation (14,30). The decrease in the ΔD value reflects the transition from an adlayer composed of soft dissipative vesicles to a more rigid and less dissipative flat bilayer.

The electrical properties of the SsLM were analyzed by evaluating the electrical resistance and capacitance of each formed layer. The obtained results were in good agreement with previously published work (14,15). The capacitance of the bare gold surface was $\sim 30 \mu\text{F cm}^{-2}$ and decreased significantly after recrystallization of S-layer protein to $\sim 22 \mu\text{F cm}^{-2}$ and to $\sim 3 \mu\text{F cm}^{-2}$ after formation of a lipid bilayer structure. The resistance, however, increased from $\sim 0.01 \text{ M}\Omega \text{ cm}^2$ for gold to $\sim 0.55 \text{ M}\Omega \text{ cm}^2$ for S-layer proteins and to $3.78 \pm 1.20 \text{ M}\Omega \text{ cm}^2$ for the lipid bilayer, as each additional layer acts as a barrier to charged molecules (14,15). However, fitting the impedance

spectra of the lipid membrane on S-layer protein resulted in a higher capacitance than that determined for the other lipid bilayers. This result may be explained by the highly hydrated subagent structure of the S-layer lattices (nearly 40 % proteins and 60 % water) as discussed in detail previously (14).

Incorporation of purified VDAC protein into SsLM

The interaction between the purified VDAC protein moieties produced by cell-free expression and the SsLM was assessed by QCM-D and EIS (Fig. 2 and 3, step 6). An important advantage of cell-free protein expression is the ability to produce the protein of interest within minutes; thus, the VDAC protein was synthesized *ad hoc* and purified immediately before each experiment. The presence of six N-terminal histidine (His) residues to form a so-called His-tag allowed the purification of the VDAC protein using nickel beads, which displayed good binding efficiency for the His-tagged proteins. The VDAC protein bound strongly to the nickel beads; therefore the bound protein was eluted in two fractions. SDS gel analysis of the two purified VDAC protein fractions revealed that the majority of the protein was recovered in the first elution fraction, although the second elution fraction contained substantial amounts of VDAC protein of greater purity (Fig. 4).

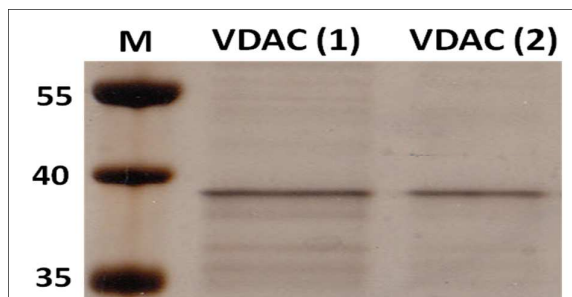


Figure 4: SDS-polyacrylamide gel electrophoresis with silver staining of two fractions of eluted VDAC protein: the first fraction was eluted in 3 M NaCl (VDAC (1)), and the second was eluted in 3 M NaCl and 500 mM imidazole in 100 mM HEPES (1:1) (VDAC (2)).

The concentration of the VDAC protein resulted in average $\sim 0.20 \text{ mg/ml}$ and $\sim 0.10 \text{ mg/ml}$ in the first and second elution fractions, respectively. In all our preparations, a prominent protein-derived signal with an apparent molecular mass of $\sim 38 \text{ kDa}$ was observed. This apparent protein mass is larger than that reported in previous studies (21,23,24), possibly due to the presence of the six His-residues.

The exposure of SsLM to 1, 2.5, and 5 $\mu\text{g/ml}$ VDAC protein resulted in small, negligible changes in the frequency and dissipation values that did not confirm VDAC protein insertion (Fig. 3). Therefore, EIS was employed to measure possible changes in membrane resistance caused by VDAC protein incorporation. Indeed, spontaneous reconstitution of the VDAC protein into the SsLM induced a significant decrease in

membrane resistance, indicating an increase in the ionic permeability of the membrane (Table 1), however, the membrane capacitance did not vary significantly. As expected, a higher VDAC protein concentration resulted in an increased number of reconstituted channels and, consequently, decreased membrane resistance.

Table 1: Membrane resistance (mean value) of the SsLM before and after interaction with purified VDAC proteins at different concentrations ($n = 3$; # $n = 2$).

Concentration ($\mu\text{g/ml}$)	0	1	2.5	5
R ($\text{M}\Omega\text{ cm}^2$)	3.78 ± 1.20	$2.59 \pm 0.62^{\#}$	2.72 ± 0.47	2.51 ± 0.90

The VDAC protein forms open channels upon reconstitution in lipid membranes. However, the gating of VDAC channels is affected by positive and negative membrane potentials as well. At low voltage ($> 10\text{ mV}$), VDAC channels are observed to be in open state, while application of high voltage ($< 10\text{ mV}$), results in the closed state. The VDAC proteins re-open once the voltage is reduced (20). This behaviour of VDAC isolated from cellular membranes had been described in literature and we could observe such characteristics in our cell – free synthesized VDAC species.

In the present study, SsLMs were exposed to purified, cell – free generated VDAC protein material with a final concentration of $5\text{ }\mu\text{g/ml}$. Currents of 0 mV , 1 mV , and 10 mV were subsequently applied to confirm voltage-dependent gating (Table 2). As observed previously, the membrane resistance dropped from the initial value of $5.12\text{ M}\Omega\text{ cm}^2$ to $3.99\text{ M}\Omega\text{ cm}^2$, which is explained by the incorporation of VDAC protein moieties into the membrane architecture. Moreover, the results indicate that starting from an applied voltage of 10 mV , the VDAC channels start to close as described in literature – resulting in an increase of the membrane resistance to $6.01\text{ M}\Omega\text{ cm}^2$. Reference measurements in which the same voltage cycle was applied to SsLMs in the absence of the VDAC protein revealed that there was no observable change in the membrane resistance. Interestingly, previous studies have shown that the channels are in the closed state at $> 10\text{ mV}$, but in the present study, the application of a very low voltage (1 mV) was sufficient to close at least a fraction of the SsLM-incorporated VDAC channels. Hence, a slightly higher resistance of $4.58\text{ M}\Omega\text{ cm}^2$ compared to $3.99\text{ M}\Omega\text{ cm}^2$ at a voltage of 0 mV was observed. While the membrane resistance decreased again after the voltage was reduced from 10 mV to 0 mV , the value was higher compared to the first measurement (in which the membrane resistance at 0 mV before and after increasing the voltage was $3.99\text{ M}\Omega\text{ cm}^2$ and $4.69\text{ M}\Omega\text{ cm}^2$, respectively) due to the re-opening of some channels while others remain closed. Indeed, injection of 10 mM NADH into the VDAC protein reconstituted in the SsLM caused a significant increase in the membrane resistance to

$6.85\text{ M}\Omega\text{ cm}^2$, which indicates blocking of VDAC channels by NADH molecules (Table 2) as to be expected.

Table 2: Membrane resistance of the SsLM before and after the addition of $5\text{ }\mu\text{g/ml}$ VDAC proteoliposomes at various applied voltages.

Applied Voltage (mV)	SsLM	Addition of VDAC protein ($5\text{ }\mu\text{g/ml}$) (Before NADH)				Addition of 10 mM NADH
	0 mV Before lysate add.	0 mV	1 mV	10 mV	0 mV*	0 mV
R ($\text{M}\Omega\text{ cm}^2$)	5.12	3.99	4.58	6.01	4.69	6.85

* After application of a voltage cycle up to 10 mV .

Synthesis of the VDAC protein in presence of the SsLM using a cell-free protein expression system

We performed synthesis of VDAC in presence of the SsLM by mixing VDAC cDNA with the cell-free reaction mixture followed by direct injection into the QCM-D chamber and incubation for a sufficient time to ensure protein expression and incorporation into the SsLM.

Injection of the cell-free lysate/VDAC cDNA caused a rapid drop in the ΔF signal down to -400 Hz . This value decreased gradually further down until a value of approximately -430 Hz was reached. The ΔF signal returned to approximately -360 Hz after the post-incubation rinsing step due to the removal of non-adsorbed material from the SsLM. The same characteristic ΔF drop was observed using a plain gold sensor instead of the SsLM covered sensor, indicating that the cell-free reaction mixture itself caused such pronounced decrease in frequency and not any specific interaction with the SsLM. QCM-D signals were in the same range - regardless of presence or absence of the cDNA, coding for VDAC. However, presence of generated VDAC protein was confirmed by a specific VDAC antibody in a western blot analysis for which the QCM-D micro-chamber was rinsed by respective loading buffer after synthesis had been performed (Fig. 5).

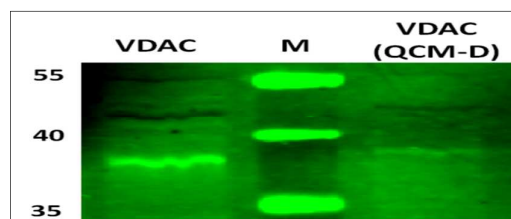


Figure 5: Western blot of VDAC protein synthesized by the cell-free system in the absence and presence of the SsLM after collecting the sample from the QCM-D chamber (VDAC (QCM-D)). A polyclonal rabbit anti-humanVDAC antibody was used for detection. The difference in the apparent molecular mass is likely due to the presence of lipid molecules, which may affect protein mobility during polyacrylamide gel electrophoresis, as has been observed for the amphiphilic family of membrane protein species in general. Absence of the VDAC expression

plasmid or addition of only 2nd antibody material did not result in any visible signal.

The results obtained confirmed that VDAC protein synthesis occurred, and they demonstrated that a duration of 30 minutes was sufficient for VDAC protein synthesis; longer incubation times had no beneficial effect on protein production.

Before adding the cell-free reaction mixture, the resistance of the SsLM was $3.27 \pm 1.27 \text{ M}\Omega \text{ cm}^2$. After addition of the cell-free reaction mixture and subsequent incubation for ~60 min, the resistance decreased to 1.49 and $2.35 \text{ M}\Omega \text{ cm}^2$ for the cell-free reaction mixtures with or without the VDAC plasmid, respectively, when no voltage (0 mV) was applied. This result might indicate not only the production of VDAC protein, as shown in Fig. 5, but also the functional incorporation of VDAC into the SsLM. Moreover, the membrane resistance increased to $3.17 \text{ M}\Omega \text{ cm}^2$ when a voltage of 20 mV was applied, indicating the known gating of the VDAC protein. A further increase in the voltage to 40 mV resulted in further decrease of the membrane resistance down to $2.09 \text{ M}\Omega \text{ cm}^2$, while adding 10 mM NADH at 0 mV to the SsLM containing the putative VDAC channels resulted in an increase in the membrane resistance to $4.67 \text{ M}\Omega \text{ cm}^2$, which can be explained by the blocking effect of NADH on VDAC channels (Table 3).

Table 3: Membrane resistance of the SsLM after the addition of cell-free reaction mixture with VDAC plasmid at various applied voltages (*n* = 2).

Applied Voltage (mV)	SsLM	Cell-free VDAC protein synthesis mixture				Addition of 10mM NADH
	0 mV Before lysate add.	0 mV	20 mV	40 mV	60 mV	
R (MΩ cm ²)	2.81±1.40	1.49±0.04	3.03±1.25	2.09±0.36	2.84±1.55	4.67±4.55

Taken together, with the ‘direct’ synthesis strategy of VDAC proteins in presence of a SsLM architecture, we could observe meaningful EIS responses as well as with the vesicle fusion strategy, summarized in Table 3. As in the biochemical analysis, presence of VDAC protein in the QCM channel was shown. Only the NADH blocking experiment was unspecific for the ‘direct’ synthesis setting as absence or presence of VDAC expression plasmid resulted in comparable EIS values.

DISCUSSION

The design of a synthetic membrane that mimics a natural membrane is extremely useful for understanding cell membrane-related processes. Therefore, the identification of a

proper matrix for the functional embedding of integral peptides or proteins comprises an area of increasing interest. One of the best-established synthetic membrane architectures is the SsLM. Lipid membranes are limited by their short longevity and low mechanical stability; however, separating the lipid-protein membrane from a solid substrate with a soft cushion overcomes these issues and provides a high-throughput platform for further investigations (31-33). The supramolecular architectural principles of an archaeal cell envelopes composed of S-layer-stabilized lipid membranes have been imitated to generate more stable functional lipid membranes with nanopatterned fluidity at meso- and macroscopic scales (7). Römer and Steinem (34) reported formation of nano-black lipid membrane (nano-BLM) on porous alumina substrate attached to solid surface. This membrane architecture shows long term and high mechanical stability and its functionality has been confirmed by inserting channel active peptides, such as gramicidin and alamethicin for electrochemical investigations.

In our the present study on the combination of SPR (data not shown), EIS and QCM-D for detailed characterization based on different characterization principles in order to obtain a most comprehensive overview on our layer architecture, VDAC insertion and functional characterization.

Previous studies have demonstrated successful production of the VDAC protein in a cell-free system (36-38), followed by integration into lipid vesicles to produce, in a one-step reaction, functional proteoliposomes that were tested in mammalian cells to measure cytochrome c release and activation of apoptosis or to measure electrophysiological activity with the patch clamp technique (36,37). Here, the functionality of the human VDAC protein reconstituted into the SsLM was examined according to two strategies. The first strategy, which utilized purified VDAC, confirmed the functional incorporation of VDAC and the formation of active channels. When reconstituted in lipid membranes, the VDAC protein forms open channels in the shape of cylindrical pores that are permeable to nearly all ions (21). As described above, the application of different voltages had a significant effect on the opening and closing of the VDAC channels. The application of a voltage followed by a decrease in voltage obviously led to changes in the channel configuration because the membrane resistance decreased after the voltage was reduced, although the value remained higher than before the application of any voltage because some channels re-opened while others remained closed. It is possible that keeping the channels in the closed state for a long time during impedance measurements may reduce the rate of channel re-opening and induce some structural rearrangements to achieve more stable closed conformations (39). These phenomena, which are reported here for the first time, can be explained by the combination of cell-free synthesized VDAC protein species with the lipid membrane architecture supported by an S-layer protein cushion.

The presence of the nucleotides NADH or NADPH induces pore closure and inhibits VDAC channel conductance, while other nucleotides (NAD⁺, ATP, ADP, cAMP, and cGMP) have no effect on the function of the channel (25,39,40). An NMR spectroscopy study identified the site of NADH binding as flanking a short Gly-X-Gly-X-Gly sequence that links the N-terminus to strand β 1 (41).

With cell free synthesis, the protein of interest, in our case the VDAC protein, is not exposed to denaturation procedures. Consequently, every synthesized VDAC protein molecule might be in direct contact with the SsLM, followed by functional incorporation. Moreover, the nascent synthesized membrane protein chain might exhibit a conformation that facilitates the incorporation process.

In our experiments, the cell free synthesis of VDAC protein into vesicles for fusion on top of a planar membrane show higher fidelity in terms of reproducibility and liability in the NADH blocking assay – we explain this phenomenon with the strong interaction of the cell lysate with the membrane architecture, resulting in partial ‘lysis’ and de-organization of the membrane architecture as the cell-free cell lysate can be considered a highly crowded and detergent-like environment. It will be important in future approaches to investigate the stabilization of the membrane architecture against the destructive influence of the cell-free lysate.

Experimental

Isolation of S-layer proteins

The S-layer protein S-layer protein with a molecular weight of 127 kDa, was isolated from *Lysinibacillus sphaericus* CCM 2177 as previously described (26). The protein solution (1 mg/ml) was diluted 1:10 prior the use with crystallization buffer (0.5 mM Tris-HCl, 10 mM CaCl₂, pH 9). Re-crystallization of S-layer proteins on the gold substrate was performed for at least 3 hours or overnight.

EDC Activation

1-ethyl-3-(3-dimethylaminopropyl) carbodiimide hydrochloride (EDC) was purchased from Sigma-Aldrich. To modify the S-layer protein, EDC (15 mg/ml, pH 4.5) was added to react with free carboxyl groups on the S-layer protein forming highly reactive O-acylisourea intermediates. Subsequently liposomes containing DMPE were bound via EDC coupling onto the S-layer protein lattice (14,27).

Vesicles Preparation and Membrane Formation

Egg yolk phosphatidylcholine (Egg PC), 1,2-dimyristoyl-sn-glycero-3-phosphoethanolamine (DMPE), were purchased from Sigma-Aldrich, and cholesterol from Avanti Polar Lipids Inc, USA. The β -diketone ligand has been synthesized as described elsewhere (28). Egg PC: DMPE: cholesterol (molar ratio 4:1:1) and 1% β -diketone ligand were dissolved in chloroform in a round bottom flask, dried under vacuum for at

least 3 hours at 45°C. The lipid film was then rehydrated in 200 mM sucrose and extruded 21 times through a 100 nm polycarbonate membrane (Whatman, UK) by using a Mini Extruder (Avanti Polar Lipid Inc, USA) to form a suspension of small unilamellar vesicles (SUVs). Before use, vesicles were diluted in 1:2 sucrose to glucose ratio to give a final lipid concentration of 1 mg/ml. Membrane formation out of the bound vesicles was performed as described elsewhere (14).

Plasmids construction

E. coli DH5 α (Invitrogen) was used for plasmid propagation. Bacteria were cultured in Luria-Bertani (LB) broth or agar at 37°C supplemented with the appropriate antibiotics; ampicillin or kanamycin at final concentration of 50 μ g/ml.

Oligonucleotide primers for the amplification of DNA fragment were designed with *attB1* or *attB2* sites for the insertion into the Gateway donor vector pDONR 221 by homologous recombination. Two different primers were designed and used in this study; one forward primer (GGGG-attB1 gc gaa gga gat aga acc ATG GCT GTG CCA CCC ACG TAT G) and one reverse primer (GGGG-attB2 t TTA CTC GAG TGC TTG AAA TTC CAG TCC). For gateway cloning, the two reactions, BP and LR, were done according to the manufacturer’s instructions (Invitrogen). Briefly, the cDNA sequence of the gene of VDAC was amplified by PCR. These PCR products were cloned into pDONR221 to create entry clones. Subsequently, the resulting plasmids were used to transfer the gene sequences into the destination vector pDEST17, which incorporates an N-terminal 6 \times His-tag into inserted genes via homologous recombination. Produced plasmids were analyzed by restriction mapping and confirmed by sequencing to ensure that no errors were introduced and then used directly for the synthesis of the VDAC protein.

Cell-free VDAC protein expression and purification

S30 T7 high yield protein expression system and MagneHisTM protein purification system were purchased from Promega, Germany. Cell-free VDAC protein synthesis reaction was assembled and incubated as recommended in the manufacturer’s instructions in respective volumes of 50 μ l. The resulting VDAC proteins were purified from the cell lysate by nickel beads according to the manufacturer’s instructions and eluted from the beads in a two-step process. A first fraction was eluted by 3M NaCl and the second one by a mixture of 3M NaCl and 500mM imidazole, 10mM HEPES (1:1). The second elution fraction was employed in all experiments since it showed higher purity than the first one in the PAGE. VDAC proteins were separated by SDS-PAGE (NuPAGE) and analyzed either by silver staining or by using rabbit anti-VDAC polyclonal antibody (Cell Signalling) as primary antibody and IRDye 680CW Goat anti-Rabbit IgG (LI-COR) as a secondary antibody. The specifically bound antibodies were visualized by LI-COR Odyssey infrared imaging system (Germany).

Quartz Crystal Microbalance with Dissipation Monitoring (QCM-D)

QCM-D (E4, QSense AB, Sweden) is used to measure the changes in frequency (ΔF), which is related to the mass of the material adsorbed on or removed from the sensor, and energy dissipation (ΔD), providing information on the viscoelastic properties of the adsorbed materials before, during, and after the interaction. The substrates used in this study are commercially available sensor crystals for the E4 system (Qsx 301, Q-Sense AB, Sweden), having a diameter 14 mm and are coated with a 100-nm thick gold film. QCM-D experiments were measured at 25 or $37 \pm 0.02^\circ\text{C}$. The flow rate for S-layer protein injection was $50 \mu\text{l/min}$ and $25 \mu\text{l/min}$ for all others fluid injections and rinsing steps.

Electrochemical Impedance Spectroscopy (EIS)

EIS measurements were performed using the Q-sense Electrochemistry Module (QEM 401, Q-Sense AB, Sweden) in connection to a potentiostat (CH Instrument, CHI660c, Austin, USA). QCM-D sensor used as a working electrode for electrochemistry measurements, a platinum counter-electrode on the top wall of the chamber, and an Ag/AgCl reference electrode is fixed in the outlet flow channel. The frequency was measured within the range of 100 mHz to 100kHz . An AC potential of 15 mV was applied at a DC voltage of 0 mV versus the used reference electrode. The used electrolyte in all experiments was 10 mM HEPES buffer, 150 mM NaCl, pH 7.4. The impedance data were fitted by the CHI software in a parallel equivalent circuit $R_{el} - R_m \text{ ZCPE}$; where R_{el} is the electrode resistance, R_m is the membrane resistance, and ZCPE is a constant phase element (CPE). The surface area specific electrolyte resistance for all formed membranes in this study was in range between $5\text{--}7 \Omega \text{ cm}^2$.

Conclusions

We present an elegant strategy of incorporation of cell-free synthesized VDAC protein species in the robust SsLM system. Incorporation of VDAC into the SsLM 2D membrane architecture is achieved *via* vesicle fusion or *via* direct synthesis as we could harvest VDAC protein from the QCMD – quartz surface, demonstrating the superior robustness of our approach. However, the strategy to form VDAC functionalized lipid vesicles allowed purification via affinity tag – followed by vesicle fusion resulted in unambiguous electrochemical responses from the incorporated VDAC channels. The combination of QCM-D and EIS allows monitoring of the layer assembly in the SsLM context as well as the reproducible functional analysis of the VDAC channels in their gating behaviour.

We conclude from the presented data, that the challenges of investigating biological systems, such as membrane proteins,

can be bypassed by re-designing and mimicking existing, natural membrane architectures using synthetic alternatives. Physiological investigations of subtle membrane proteins, such as the human VDAC protein species, can be achieved by the cell free synthesis and incorporation protocol reported here. Using highly sensitive biophysical techniques such as QCM-D and EIS, the VDAC protein was studied in such robust environment such as the SsLM, illustrating the potential of this approach for developing a biosynthetic architecture with engineered properties that promote stability and reproducibility and at the same time, our approach allows access to the family of membrane proteins, being notoriously difficult to handle in the complexity of a living cell.

Acknowledgements

We thank Christian Stanetty (Department of Chemistry, University of Natural Resources and Life Sciences, Vienna, (BOKU) Austria) for the chemical synthesis of the β -diketone ligand, Erik Reimhult and Christian Zafiu (Department of Nanobiotechnology, (BOKU) Austria) for their kind help and advices on QCM-D and EIS measurements, Sebastian Giehling and Jörg Eisfeld (Nanospot GmbH, Münster- Germany) for useful discussion and helping with measuring the membrane stability.

Notes and references

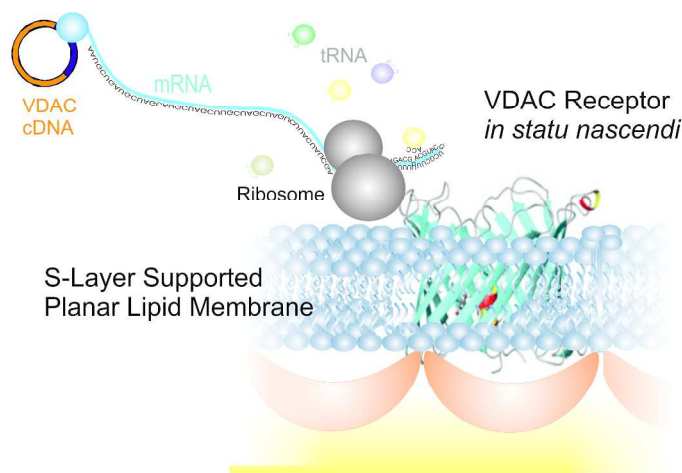
ABBREVIATIONS

D dissipation; F frequency; EIS electrochemical impedance spectroscopy; QCM-D quartz crystal microbalance with dissipation monitoring; S-layer protein S-layer proteins; SsLM S-layer-supported lipid membrane; VDAC voltage-dependent anion channel.

REFERENCES

- Naumann, R.; Jonczyk, A.; Kopp, R.; Vanesch, J.; Ringsdorf, H.; Knoll, W.; Graber, P. *Angew. Chem.* **1995**, *34*, 2056-2058.
- Lipowsky, R. and Sackman, E. *Handbook of Biological Physics*. Elsevier, North-Holland, Amsterdam, **1995**.
- Belegriou, S.; Menon, S.; Dobrunz, D.; Meier, W. *Soft Matter*. **2011**, *7*, 2202-2210.
- Seddon, A.; *et al.*, *Chem. Soc. Rev.* **2009**, *38*, 2509-2519.
- Rossi, C. and Chopineau, J. *Eur. Biophys. J.* **2007**, *36*, 955-965.
- Jackman, J.; Knoll, W.; Cho, N. *Materials*. **2012**, *5*, 2637-2657.
- Schuster, B. and Sleytr, U.B. *J. Struct. Biol.* **2009**, *168*, 207-216.
- Sleytr, U.B.; Messner, P.; Pum, D.; Sára, S. M. *Angew. Chem. Int. Ed.* **1999**, *38*, 1034-1054.
- Sleytr, U.; *et al.*, *FEMS Microbiol. Rev.* **2014**, *38*, 823-864.
- Albers, S. and Meyer, B. *Nat. Rev. Microbiol.* **2011**, *9*, 414-426.
- Gufier, P.; Pum, D.; Sleytr, U.B.; Schuster, B. *Biochim Biophys Acta – Biomembranes*. **2004**, *1661*, 154-165.

- 12 Schuster, B.; Gufler, P.; Pum, D.; Sleytr, U.B. *IEEE Trans Nanobiosci.* **2004**, 3, 16–21.
- 13 Schuster, B. and Sleytr, U. *J. R. Soc. Interface.* **2014**, 11, 20140232.
- 14 Schrems, A.; Larisch, V.; Stanetty, C.; Dutter, K.; Damiaty, S.; Sleytr, U.; Schuster, B. *Soft Matter.* **2011**, 7, 5514–5518.
- 15 Schrems, A.; Kibrom, A.; Kupcu, S.; Kiene, E.; Sleytr, U.; Schuster, B. *Langmuir.* **2011**, 27, 3731–3738.
- 16 Sinner, E.; *et al.*, *Materials Today.* **2010**, 13, 46–55.
- 17 Chalmeau, J.; *et al.*, *Biochem. et Biophysic. Acta.* **2011**, 1808, 271–278.
- 18 Katzen, F.; Peterson, T.; Kudlicki, W. *Trends Biotech.* **2009**, 27, 455–460.
- 19 Schwarz, D.; *et al. Methods.* **2007**, 41, 355–369.
- 20 Colombini, M. *Nature.* **1979**, 279, 643–645.
- 21 Colombini, M. *Mol. Cell. Biochem.* **2004**, 256, 107–115.
- 22 Malia, T.; Wagner, G. *Biochem.* **2007**, 46, 514–525.
- 23 Hiller, S.; *et al.*, *Science.* **2008**, 321, 1206–1210.
- 24 Raschle, T.; *et al. J. Am. Chem. Soc.* **2009**, 131, 17777–17779.
- 25 Zizi, M.; *et al. J. Biol. Chem.* **1994**, 269, 1614–1616.
- 26 Sleytr, U.B.; *et al. Arch. Microbiol.* **1986**, 146, 19–24.
- 27 Göbel, C.; *et al.*, *Colloids. Surf. B Biointerfaces.* **2010**, 75, 565–572.
- 28 Marchi-Artzner, V.; *et al.*, *Chem. Eur. J.* **2004**, 10, 2342–2350.
- 29 Haluska, C.; *et al. PNAS.* **2006**, 103, 15841–15846.
- 30 Reimhult, E.; Höök, F.; Kasemo, B. *Langmuir.* **2003**, 19, 1681–1691.
- 31 Sackmann, E. and Tanaka, M. *Trends in Biotech.* **2000**, 18, 58–64.
- 32 Castellana, E. and Cremer, P. *Surf. Sci. Rep.* **2006**, 61, 429–444.
- 33 Früh, V.; Ijzerman, A.; Siegal, G. *Chem. Rev.* **2011**, 111, 640–56.
- 34 Römer, W. and Steinem, C. *Biophysical J.* **2004**, 86, 955–965.
- 35 Damiaty, S.; Schrems, A.; Sinner, E-K.; Sleytr, U.; Schuster, B. *Int. J. Mol. Sci.* **2015**, 16, 2824–2838.
- 36 Liguori, L.; Marques, B.; Villegas-Mendez, A.; Rothe, R.; Lenormand, J. *J. Control. Rel.* **2008**, 126, 217–227.
- 37 Varnier, A.; Kermarrec, F.; Blesneac, I.; Moreau, C.; Liguori, L.; Lenormand, J. *N. J. Membr. Biol.* **2010**, 233, 85–92.
- 38 Nguyen, T.; Lieu, S.; Chang, G. *J. Mol. Microbiol. Biotechnol.* **2010**, 18, 85–91.
- 39 Colombini, M.; Blachly-Dyson, E.; Forte, M. *Ion Channels.* **1996**, 4, 169–202.
- 40 Lemasters, J. and Holmuhamedov, E. *Biochem. et Biophys. Acta.* **2006**, 1762, 181–190.
- 41 Ujwal, R.; *et al. Proc. Natl. Acad. Sci.* **2008**, 105, 17742–17747.
- 42 Györfvay, E.; Wetzler, B.; Sleytr, U.B.; Sinner, A.; Offenhäusser, A.; Knoll, W. *Langmuir.* **1999**, 15, 1337–1339.



Scheme of the cell-free, ribosomal synthesis of a VDAC protein in the presence of an S-layer supported lipid membrane. The VDAC protein is adapted from Hiller, S.; et al., Science. 2008, 321, 1206-1210
325x152mm (300 x 300 DPI)